

RSC Advances



This is an *Accepted Manuscript*, which has been through the Royal Society of Chemistry peer review process and has been accepted for publication.

Accepted Manuscripts are published online shortly after acceptance, before technical editing, formatting and proof reading. Using this free service, authors can make their results available to the community, in citable form, before we publish the edited article. This *Accepted Manuscript* will be replaced by the edited, formatted and paginated article as soon as this is available.

You can find more information about *Accepted Manuscripts* in the [Information for Authors](#).

Please note that technical editing may introduce minor changes to the text and/or graphics, which may alter content. The journal's standard [Terms & Conditions](#) and the [Ethical guidelines](#) still apply. In no event shall the Royal Society of Chemistry be held responsible for any errors or omissions in this *Accepted Manuscript* or any consequences arising from the use of any information it contains.

ARTICLE

Sulfanilic acid-functionalized silica-coated magnetite nanoparticles as an efficient, reusable and magnetically separable catalyst for the solvent-free synthesis of 1-amido- and 1-aminoalkyl-2-naphthols

Cite this: DOI: 10.1039/x0xx00000x

Received 00th January 2012,
Accepted 00th January 2012

DOI: 10.1039/x0xx00000x

www.rsc.org/

H. Moghanian,^{a*} A. Mobinikhaledi,^b A. G. Blackman,^c E. Sarough-Farahani^b

Sulfanilic acid-functionalized silica-coated nano-Fe₃O₄ particles (MNPs-PhSO₃H) have been prepared as a reusable heterogeneous acid catalyst using a facile process. The catalytic performance of this novel material has been studied in the synthesis of 1-amido- and 1-aminoalkyl-2-naphthol derivatives via a one-pot three-component condensation reaction of aldehydes, 2-naphthol, and amides/urea/amines in good to excellent yields, under solvent-free classical heating conditions. The catalyst was easily separated from the reaction mixture with the assistance of an external magnetic field and reused for several consecutive runs without significant loss of its catalytic efficiency. Results obtained from transmission electron microscopy (TEM), scanning electron microscope (SEM), powder X-ray diffraction (XRD) and sample magnetometry (VSM) show that the synthesized magnetic nanocomposites are superparamagnetic with a size range of 15-30 nm.

1. Introduction

Multicomponent reactions (MCRs) are of increasing importance in organic synthesis for building diverse and complex organic molecules through tandem carbon-carbon and carbon-heteroatom bond formation.¹⁻⁵ Advantages of these reactions include the use of simple procedures, time and energy efficiency, high bond formation yields and low cost.⁶ The development of one-pot MCRs and the improvement of known MCRs are areas of research which have attracted considerable attention in recent years.^{7, 8} One of these MCRs is the preparation of amidoalkyl naphthols. Amidoalkyl naphthols having 1,3-amino-oxygenated functional groups exist in a variety of biologically significant natural products as well as in drugs including a number of nucleosides, antibiotics and HIV protease inhibitors, such as lipinavir and ritonavir.⁹⁻¹¹ It is worth to noting that 1-amidoalkyl-2-naphthols can be easily converted to 1-aminoalkyl-2-naphthol derivatives, which shows important biological activities like depressor and bradycardiac effect^{12, 13} by amide hydrolysis reactions. These 1-aminoalkyl alcohol-type ligands have been used for both asymmetric synthesis and catalysis.^{14, 15} Thus, due to their biological, medicinal and pharmacological importance, many procedures have been developed for the preparation of 1-amidoalkyl-2-naphthols from aldehydes, 2-naphthols, and amides or urea under thermal heating and sonication conditions using catalysts such as pTSA,¹⁶ montmorillonite K10,¹⁷ iodine,¹⁸ Fe(HSO₄)₃,¹⁹ N,N,N',N'-tetrabromobenzene-1,3-disulphonamide [TBBDA],²⁰ SnCl₄·5H₂O,²¹ H₄SiW₁₂O₄₀,²² dodecylphosphonic acid,²³ cyanuric chloride,²⁴ Bi(NO₃)₃·5H₂O,²⁵ ZrO(OTf)₂,²⁶ P₂O₅,²⁷ thiamine hydrochloride,²⁸ HClO₄-SiO₂,²⁹ cation-exchange resins,³⁰ silica sulfuric acid,³¹ zwitter

ionic salts³² and Brønsted acidic ionic liquids.³³ However, some of these methods are not environmentally friendly and suffer from one or more limitations, such as prolonged reaction times, high reaction temperature, low yields of the desired product, tedious work-up, toxicity, and poor recovery and reusability of the catalyst. Therefore, a great demand still exists for versatile, simple, and environmentally friendly processes for the synthesis of 1-amido- or 1-aminoalkyl-2-naphthols under simple and practical conditions.

Organic-inorganic hybrid materials as heterogeneous catalyst have received much recent attention as they permit mutual advantages of both homogeneous as well as heterogeneous catalysts in organic synthesis.³⁴⁻³⁷ In this context, the use of nanoparticles as heterogeneous catalyst supports have received increasing attention because their small diameters provide large external surface areas for catalysis, which allows a high dispersion of the active species and provides a large amount of the active and accessible centers.³⁸⁻⁴⁰ However, tedious recovery procedures via filtration or centrifugation and the inevitable loss of solid catalysts in the separation process have limited their application.

In recent years, magnetic nanoparticles (MNPs) (e.g. Fe₃O₄) have been extensively investigated as inorganic catalyst supports in the synthesis of organic-inorganic hybrid catalysts, because of their good stability, easy synthesis and functionalization and high surface area, as well as low toxicity and price.^{41, 42} An important feature of these nano-catalysts is their separation from the reaction mixture using an external magnet, thereby obviating the need for filtration. However, magnetic nanoparticles can easily aggregate into larger clusters, due to anisotropic dipolar attraction, and thereby lose their dispersibility and catalytic activity.⁴³ In addition, Fe₃O₄

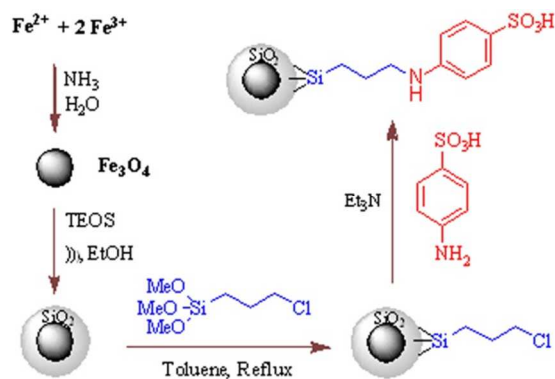
nanoparticles undergo reactions in an acid environment which lead to loss of their magnetic properties, and thus often require coating with a protective shell of silica to form a core-shell ($\text{Fe}_3\text{O}_4@\text{SiO}_2$) structure. The silica shell can prevent the aggregation of the Fe_3O_4 particles and provide numerous surface Si-OH groups for further modification.^{44,45}

With the aim of developing a more efficient synthetic process, herein, we report the synthesis of a new silica-coated Fe_3O_4 nanoparticle-supported sulfanilic acid (MNPs-PhSO₃H) and its application as an inexpensive, highly efficient and magnetically recoverable catalyst for the synthesis of 1-amido- or aminoalkyl naphthol via the one-pot three-component reaction of β -naphthol, aldehydes, and amides/urea/amines under solvent-free classical heating conditions.

2. Results and discussion

2.1. Preparation and characterization of the catalyst

The magnetic nanoparticle supported sulfanilic acid catalyst (MNPs-PhSO₃H) was prepared following the procedure shown in Scheme 1. Magnetite (Fe_3O_4) nanoparticles were easily prepared via the chemical co-precipitation of Fe^{2+} and Fe^{3+} ions in basic solution. These were subsequently coated with silica ($\text{Fe}_3\text{O}_4@\text{SiO}_2$) through the well-known Stober method.⁴⁶ The $\text{Fe}_3\text{O}_4@\text{SiO}_2$ core-shell structures were then sequentially treated with 3-chloropropyltriethoxysilane (CPTS), which can bind covalently to the free-OH groups at the surface of the particles. Finally, reaction of the 3-chloropropyl-functionalized magnetic silica nanoparticles ($\text{Fe}_3\text{O}_4@\text{SiO}_2\text{-Cl}$) with sulfanilic acid gives the sulfanilic acid-functionalized silica-coated magnetite nanoparticles (MNPs-PhSO₃H).



Scheme 1 Preparation of sulfanilic acid-functionalized silica-coated nano- Fe_3O_4 particles.

The as-prepared catalyst was also characterized by Fourier transform infrared spectroscopy (FTIR), X-ray diffraction (XRD), field emission scanning electron microscopy (FE-SEM), transmission electron microscopy (TEM), the energy dispersive X-ray (EDX), vibrating sample magnetometry (VSM), and thermogravimetric analysis (TGA). Figure 1 shows the FT-IR spectrum of Fe_3O_4 , $\text{Fe}_3\text{O}_4@\text{SiO}_2$, $\text{Fe}_3\text{O}_4@\text{SiO}_2\text{-Cl}$, and MNPs-PhSO₃H nanoparticles in the wavenumber range 4000–400 cm^{-1} . The FT-IR spectrum of the MNPs was similar to those of Fe_3O_4 materials described in the literature. FT-IR spectra of the bare magnetic Fe_3O_4 nanoparticles displayed the characteristic Fe-O absorption around 575 cm^{-1} (Fig. 1a).

$\text{Fe}_3\text{O}_4@\text{SiO}_2$ shows characteristic IR absorption bands at about 1090, 950, 800 and 465 cm^{-1} which are attributed to the asymmetric stretching, symmetric stretching, in plane bending and rocking mode of the Si–O–Si group, respectively. These results confirm the presence of SiO_2 . The broad peaks in the range 3200–3500 cm^{-1} and the weak peak at 1620 cm^{-1} are due to the O–H stretching vibration mode (Si–OH) and twisting vibration mode of H–O–H adsorbed in the silica shell, respectively. The presence of the anchored alkyl groups is confirmed by the weak aliphatic C–H symmetric and asymmetric stretching vibrations at 2926 and 2963 cm^{-1} in figure 1c and 1d. Thus the above results indicate that the functional groups were successfully grafted onto the surface of the magnetic $\text{Fe}_3\text{O}_4@\text{SiO}_2$ nanoparticles.

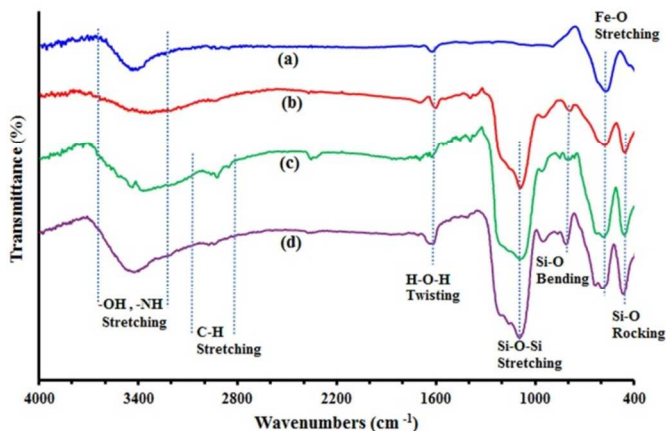


Fig. 1 The comparative FT-IR spectra for (a) Fe_3O_4 , (b) $\text{Fe}_3\text{O}_4@\text{SiO}_2$, (c) $\text{Fe}_3\text{O}_4@\text{SiO}_2\text{-Cl}$ and (d) MNPs-PhSO₃H.

The nanoparticle size and morphology of MNPs-PhSO₃H catalyst were investigated by field emission scanning electron microscopy (FE-SEM) (Fig. 2). As can be seen from Fig. 2, MNPs-PhSO₃H particles have a mean diameter of about 15–35 nm and a nearly spherical shape. The energy dispersive X-ray spectroscopy (EDS) results, obtained from SEM analysis of MNPs-PhSO₃H, are shown in Fig. 3, and clearly show the presence of S in the MNPs-PhSO₃H catalyst. Moreover, the presence of Si, O, and Fe signals indicates that the iron oxide particles are loaded into silica, and the higher intensity of the Si peak compared with the Fe peaks indicates that the Fe_3O_4 nanoparticles were trapped by SiO_2 . According to the above analysis, it can be concluded that the MNPs-PhSO₃H have been successfully synthesized. In addition, TEM analysis shows a dark nano- Fe_3O_4 core surrounded by a grey silica shell about 5–10 nm thick and the average size of the obtained particles is 15–30 nm (Fig. 4).

The presence as well as the degree of crystallinity of magnetic Fe_3O_4 and the MNPs-PhSO₃H catalyst was obtained from XRD measurements (Fig. 5). The same peaks were observed in the both of the MNPs and MNPs-PhSO₃H XRD patterns, indicating retention of the crystalline spinel ferrite core structure during the silica-coating process. The XRD data of the synthesized magnetic nanoparticles show diffraction peaks at $2\theta = 30.4^\circ$, 35.7° , 43.3° , 53.9° , 57.3° , 63.0° , and 74.5° which can be assigned to the (220), (311), (400), (422), (511), (440) and (533) planes of Fe_3O_4 , respectively, indicating that the Fe_3O_4 particles in the nanoparticles were pure Fe_3O_4 with a cubic spinel structure; these match well with the standard Fe_3O_4 sample (JCPDS card No.85-1436). The broad peak from $2\theta =$

20° to 27° (Fig. 2b) is consistent with an amorphous silica phase in the shell of the silica-coated Fe_3O_4 nanoparticles ($\text{Fe}_3\text{O}_4@\text{SiO}_2$).⁴⁷

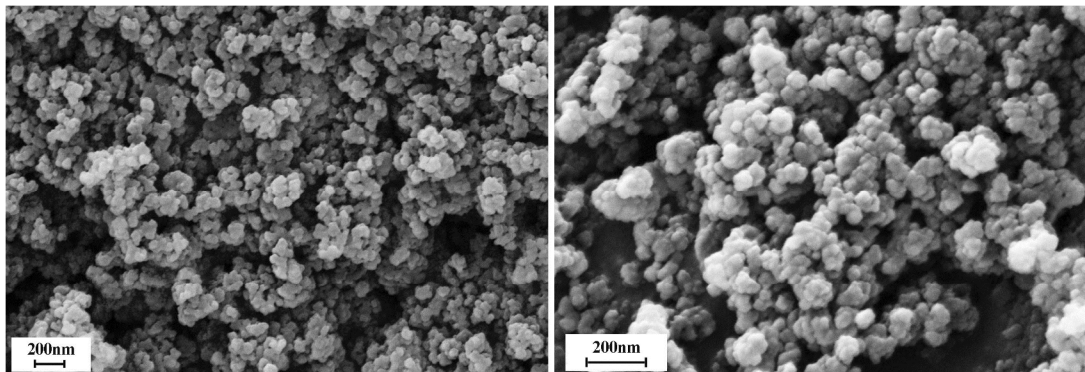


Fig. 2 FE-SEM images of MNPs- PhSO_3H nanoparticles.

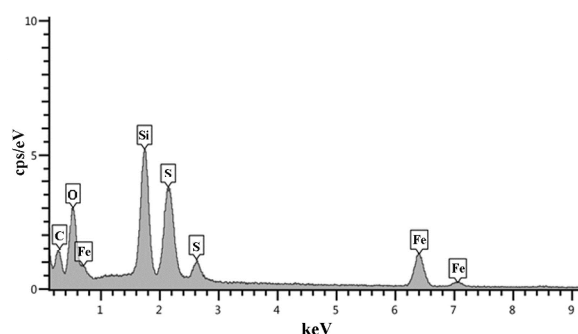


Fig. 3 EDS spectra of MNPs- PhSO_3H nanoparticles.

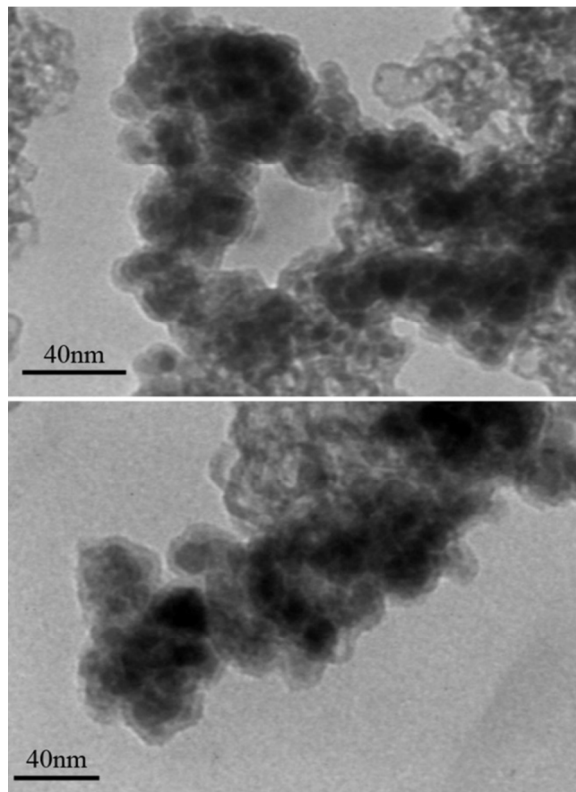


Fig. 4 TEM image of MNPs- PhSO_3H nanoparticles.

The (311) XRD peak was used to estimate the average crystallite size of the magnetic nanoparticles by Scherrer's formula ($D = 0.9\lambda/\beta\cos\theta$), where D is the average crystalline size, λ is the X-ray wave-length (0.154 nm), β denotes the full width in radians subtended by the half maximum intensity width of the (311) powder peak, and θ corresponds to the Bragg angle of the (311) peak in degrees.⁴⁸ From the width of the peak at $2\theta = 35.7^\circ$ (311), the crystallite size of the magnetic nanoparticle is calculated to be 14.7 nm using Scherrer's equation, which is smaller than the size determined by FE-SEM and TEM analysis (Fig.2 and Fig. 4). The observed difference can be attributed to the fact that XRD measurements consider crystallite sizes as sizes of "coherently diffracting domains" of crystals while grains may contain several of these domains.

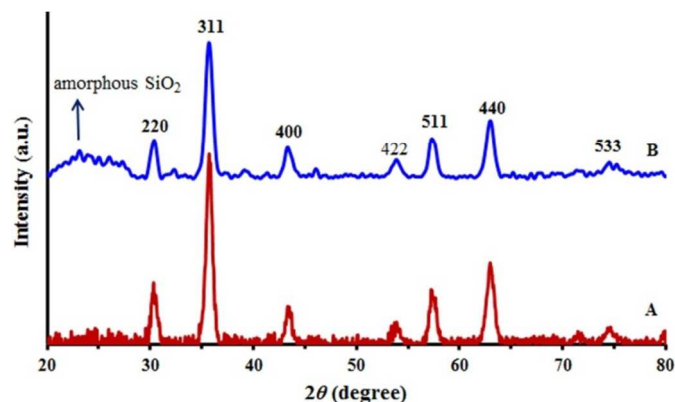


Fig. 5 XRD diffraction pattern of Fe_3O_4 MNPs (a), and $\text{Fe}_3\text{O}_4@\text{SiO}_2$ - PhSO_3H MNPs (b)

The stability of the MNPs- PhSO_3H catalyst was determined by thermogravimetric analysis (TGA) and derivative thermogravimetry (DTG) (Fig. 6). The magnetic catalyst shows two weight loss steps over the temperature range of TG analysis (Fig. 6). The first stage, including a low amount of weight loss at $T < 250^\circ\text{C}$, is due to the removal of physically adsorbed solvent and surface hydroxyl groups, and the second step at about 300°C to nearly 550°C is attributed to the decomposition of the coating organic layer in the nanocomposite. Therefore, the weight loss between 300 - 550°C gives the organic grafting ratios of the magnetic catalyst. The

grafted sulfanilic acid on the magnetic $\text{Fe}_3\text{O}_4@\text{SiO}_2$ nanoparticles was approximately 15.5 wt%. In accordance with this mass loss, it was calculated that 0.72 mmol of sulfanilic acid was loaded on 1g of MNPs-PhSO₃H catalyst. The weight loss over the range 300-370 °C could be mainly attributed to the evaporation and subsequent decomposition of SO₃H groups. Furthermore, the DTG curve shows that the decomposition of the organic structure mainly occurred at 460 °C. Therefore, the MNPs-PhSO₃H is stable around or below 300 °C. The agreement between the acid amount of MNPs-PhSO₃H (0.65 mmol/g) measured by back titration using HCl and the organic group loading determined by TGA (0.72 mmol/g), is clear evidence that the sulfonic acid groups are principally located on the surfaces of $\text{Fe}_3\text{O}_4@\text{SiO}_2$ nanoparticles, where they are accessible for adsorption and catalytic reaction processes.

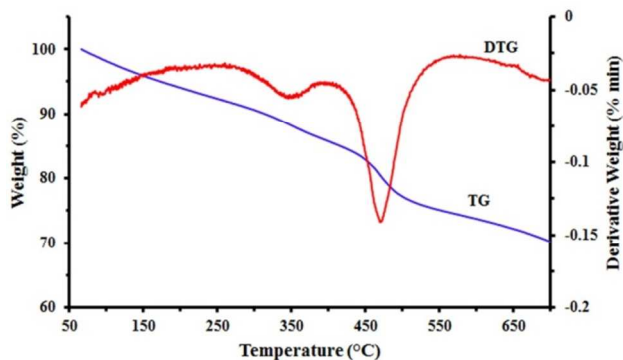


Fig. 6 TG-DTG analyses for MNPs-PhSO₃H nanoparticles.

The magnetic properties of the nanoparticles were characterized using a vibrating sample magnetometer (VSM). Figure 7 shows the plots of room temperature magnetization (*M*) versus magnetic field (*H*) (*M*-*H* curves or hysteresis loops) of Fe_3O_4 and MNPs-PhSO₃H nanoparticles. The hysteresis curve allows determination of the saturation magnetization (*M_s*), remanent magnetization (*M_r*) and coercivity (*H_c*). The magnetization of samples could be completely saturated at high fields of up to

± 8000.0 Oe and the *M_s* of samples changed from 57.6 to 38.5 emu g⁻¹, due to the formation of a silica shell around the Fe_3O_4 core. The hysteresis loops show the super-paramagnetic behavior of the Fe_3O_4 and MNPs-PhSO₃H particles in which the *M_r* and the *H_c* are close to zero (*M_r* = 0.85 and 0.45 emu g⁻¹, and *H_c* = 4.90 and 4.0 Oe, respectively).⁴⁹ The strong magnetization of the nanoparticles was also revealed by simple attraction with an external magnet (Fig. 7).

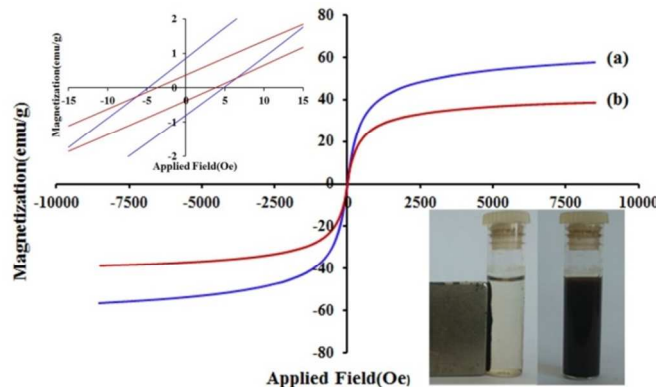
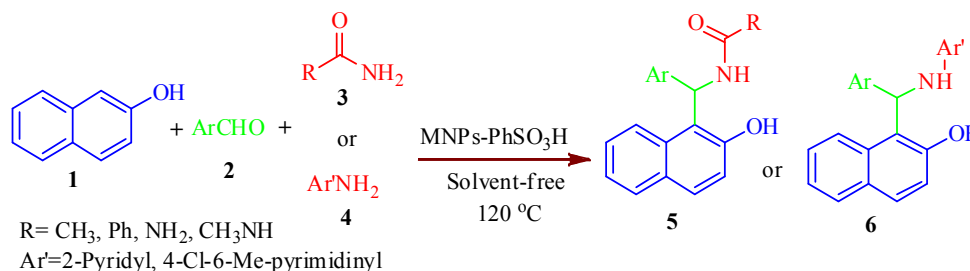


Fig. 7 The magnetic hysteresis loops of Fe_3O_4 MNPs (a), and MNPs-PhSO₃H (b). Left inset: the magnified field from -15 to 15 Oe. Right inset: the picture displays the catalyst was dispersed in liquid and captured by the outer magnet.

2.2. Synthesis of 1-Amido or aminoalkyl-2-naphthols using MNPs-PhSO₃H

After the characterization of the MNPs-PhSO₃H catalyst, its role as a catalyst was evaluated for the synthesis of 1-amido- or aminoalkyl-2-naphthols (Scheme 2).



Scheme 2 Synthesis of 1-amido- and 1-aminoalkyl naphthols.

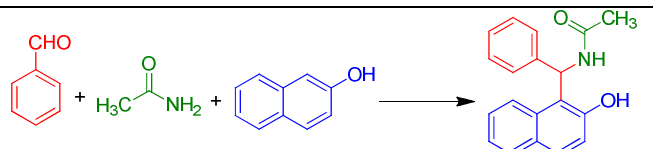
An important feature of these nano-catalysts is simple separation of them using an external magnet, thereby removing the necessity for filtration or centrifugation. In order to optimize the reaction conditions and obtain the best catalytic activity, the reaction of benzaldehyde (1 mmol), β -naphthol (1 mmol), and acetamide (1.2 mmol) was used as a model, and was conducted under different reaction parameters such as solvent and amount of catalyst. Initially, the model reaction was carried out in several solvents as well as under solvent-free conditions, to investigate the efficiency of the catalyst (Table 1). As shown in Table 1, it was found that conventional heating

at 120 °C under solvent-free conditions is more efficient than using organic solvents, with respect to reaction time and yield of the desired amidoalkyl naphthol (Table 1, entry 7). Indeed in many cases, solid organic reactions occurred efficiently and more selectively than those of their solution counterparts. To investigate the effect of catalyst loading, the model reaction was carried out in the presence of different amounts of catalyst. The best result was obtained in the presence of just 20 mg of MNPs-PhSO₃H (Table 1, entries 7-9). Moreover, the catalyst is essential and in the absence of the catalyst, only 10 % of the corresponding amidoalkyl naphthol was produced even after

prolonged reaction times (Table 1, entry 10). The efficiencies of Fe_3O_4 , $\text{Fe}_3\text{O}_4@\text{SiO}_2$ and MNPs-Cl as the catalyst towards the model reaction were compared and the results are depicted in Table 1. It was observed that the MNPs- PhSO_3H was more

efficient than the Fe_3O_4 , $\text{Fe}_3\text{O}_4@\text{SiO}_2$ and MNPs-Cl catalysts (entries 11-13).

Table 1. Optimization of the conditions for synthesis of *N*-((2-hydroxynaphthalen-1-yl)(phenyl)methyl)acetamide (Table 2, entry 1)^a.



Entry	Catalyst (mg)	Solvent	Condition	Time	Yield (%) ^b
1	MNPs- PhSO_3H (20)	THF	R.T.	24 h	20
2	MNPs- PhSO_3H (20)	THF	Reflux	12 h	32
3	MNPs- PhSO_3H (20)	EtOH	Reflux	12 h	15
4	MNPs- PhSO_3H (20)	CH_3CN	Reflux	12 h	22
5	MNPs- PhSO_3H (20)	n-Hexane	Reflux	12 h	<10
6	MNPs- PhSO_3H (20)	-	80 °C	4 h	75
7	MNPs- PhSO_3H (20)	-	120 °C	40 min	94
8	MNPs- PhSO_3H (10)	-	120 °C	40 min	79
9	MNPs- PhSO_3H (40)	-	120 °C	40 min	94
10	-	-	120 °C	4h	<10
11	Fe_3O_4 (20)	-	120 °C	3 h	54
12	$\text{Fe}_3\text{O}_4@\text{SiO}_2$ (20)	-	120 °C	3h	45
13	MNPs-Cl (20)	-	120 °C	3h	40

^a Benzaldehyde (1 mmol), 2-naphthol (1 mmol), acetamide (1.2 mmol).

^b Isolated yields.

In order to determine the generality and efficacy of the catalyst, different kinds of aldehyde carrying either electron-donating or electron-withdrawing groups were reacted with 2-naphthol, and a number of structurally and electronically diverse amides or urea, under the optimized reaction conditions; the respective results are summarized in Table 2. All reactions proceeded efficiently in the presence of catalytic amounts of MNPs- PhSO_3H at 120 °C and the desired products were obtained in good to excellent yields (87-96%) in relatively short reaction times, without formation of any side products such as dibenzoxanthenes, which are normally observed in the presence of strong acids. As can be seen in Table 2, the procedure was highly effective and the nature of substituents on the aromatic ring of aldehydes did not show obvious effects in terms of yields and times under the reaction conditions. Furthermore, when compared to the amides, *N*-methylurea afforded the corresponding amidoalkyl naphthol using shorter reaction times (Table 2, entries 10-13). The acid sensitive substrate thiophene-2-carbaldehyde gave the expected 1-amidoalkyl-2-naphthol **5e** in very good yield (Table 2, entry 5). However, when some aliphatic aldehydes, such as propionaldehyde and isobutyraldehyde, were used in this protocol under the above optimized conditions, only trace amounts of product were detected.

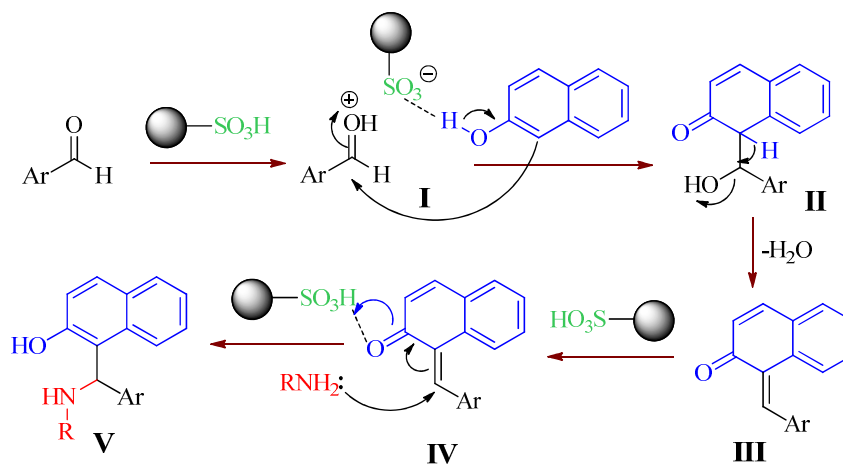
In order to show the efficiency of this catalytic system further, the synthesis of 1-aminoalkyl-2-naphthols was investigated in the presence of MNPs- PhSO_3H . As shown in Table 2, treatment of a variety of aldehydes and 2-naphthol with heterocyclic amines such as 2-aminopyridine and 2-amino-4-chloro-6-

methylpyrimidine in the presence of catalytic amounts of MNPs- PhSO_3H under the optimized reaction conditions afforded the corresponding 1-aminoalkyl-2-naphthol derivatives in 81-92% yields (Table 2, entries 18-23). However, all our attempts with the usual aromatic amines such as aniline and *p*-toluidine failed to yield the corresponding aminoalkyl naphthols. Instead, the Schiff base was prepared from the reaction of these amines and aldehydes under the reaction conditions.

A plausible mechanism for the formation of 1-amido- or 1-aminoalkyl-2-naphthols catalyzed by MNPs- PhSO_3H , which is supported by the literature,^{50, 51} is shown in Scheme 3. The MNPs- PhSO_3H catalyst participates in the reaction which activates the carbonyl group of the aldehyde (intermediate I) followed by the nucleophilic addition of β -naphthol to obtain complex II. The removal of water from complex II produces intermediate III as an ortho-quinone methide (*o*-QM). MNPs- PhSO_3H again activates intermediate III to give IV as a Michael acceptor. The activated *o*-QM then reacts with amides, amines or urea via a Michael addition to afford the expected amidoalkyl naphthols. The reaction results from amines, which have been presented in Table 2 (entries 18-23), confirm the mechanism. The reaction of usual aromatic amines such as aniline and *p*-toluidine produced the stable Schiff base and *o*-QMs were not formed under the reaction conditions. Conversely, the Schiff bases obtained from amides or heterocyclic amines are unstable and can be easily converted to starting material by a hydrolysis reaction. Thus, this reaction can proceed via the *o*-QMs intermediate.

Table 2. Synthesis of amido or aminoalkyl naphthols in the presence of MNPs-PhSO₃H under solvent-free conditions.

Entry	Ar	R or Ar'	Product	Time (min)	Yield (%) ^a	M.P. (°C)	
						Found	Reported ^{Lit.}
1	C ₆ H ₅	CH ₃	5a	40	94	241-242	238-240 ⁵²
2	4-ClC ₆ H ₄	CH ₃	5b	30	96	221-223	220-222 ⁵²
3	4-BrC ₆ H ₄	CH ₃	5c	30	93	226-227	228-230 ¹⁹
4	4-MeC ₆ H ₄	CH ₃	5d	40	89	212-213	214-216 ³³
5	2-Thiophine	CH ₃	5e	30	90	220-222	224-225 ⁵³
6	C ₆ H ₅	NH ₂	5f	25	91	178-179	177-179 ²⁵
7	3-MeOC ₆ H ₄	NH ₂	5g	45	87	238-240	241-243 ⁵⁴
8	3-NO ₂ C ₆ H ₄	NH ₂	5h	25	89	185-186	183-185 ⁵²
9	2-ClC ₆ H ₄	NH ₂	5i	35	88	152-153	150-152 ⁵⁵
10	C ₆ H ₅	CH ₃ NH	5j	12	92	192-193	190-191 ⁵⁶
11	3-NO ₂ C ₆ H ₄	CH ₃ NH	5k	10	94	195-197	191-192 ³⁰
12	4-MeC ₆ H ₄	CH ₃ NH	5l	12	93	175-176	174-176 ⁵⁶
13	4-FC ₆ H ₄	CH ₃ NH	5m	15	91	174-175	176-177 ³⁰
14	C ₆ H ₅	Ph	5n	25	90	234-235	236 ⁵⁰
15	4-ClC ₆ H ₄	Ph	5o	30	91	176-177	178-180 ⁵²
16	4-BrC ₆ H ₄	Ph	5p	40	86	183-184	182-184 ³³
17	3-NO ₂ C ₆ H ₄	Ph	5q	35	91	232-234	230-233 ⁵¹
18	C ₆ H ₅	2-Pyridyl	6r	10	92	174-176	-
19	4-ClC ₆ H ₄	2-Pyridyl	6s	15	85	181-182	-
20	C ₆ H ₅	4-Cl-6-Me-2-pyrimidinyl	6t	15	86	160-162	-
21	4-ClC ₆ H ₄	4-Cl-6-Me-2-pyrimidinyl	6u	20	88	185-186	-
22	2-Cl-6-F-C ₆ H ₃	4-Cl-6-Me-2-pyrimidinyl	6v	25	81	170-172	-
23	2-ClC ₆ H ₄	4-Cl-6-Me-2-pyrimidinyl	6w	20	83	182-184	-

^a Isolated yields.**Scheme 3** Possible mechanism for the synthesis of amido or aminoalkyl naphthols using MNPs-PhSO₃H

To compare the applicability and the efficiency of our catalyst with the reported inorganic or organic catalysts for the synthesis of 1-amidoalkyl-2-naphthols, we have tabulated the results of these catalysts in the condensation reaction of benzaldehyde, β -naphthol and acetamide under optimized conditions in Table 3. This shows that the MNPs-PhSO₃H is a moderately good catalyst for this reaction in terms of short reaction times and simple conditions and it could be considered as one of the best choices as an environmentally benign and user-friendly catalyst. Also, it can be seen that, in addition to having the general advantages attributed to the inherent magnetic properties of nano-catalysts, MNPs-PhSO₃H is an equal or more efficient catalyst for this three-component reaction.

2.3. Catalyst recovery and reuse

The recovery and reusability of the catalyst are very important for commercial and industrial applications as well as green process considerations. Thus, the recovery and reusability of MNPs-PhSO₃H (20 mg) was investigated in the sequential reaction of 3-nitrobenzaldehyde (1 mmol) with 2-naphthol (1 mmol) and N-methylurea (1.2 mmol) under solvent-free conditions for 10 min at 120 °C. After completion of the reaction, the resulting solidified mixture was diluted with hot THF (10 mL). Then, the catalyst was easily separated using an external magnet, washed with THF, dried under vacuum and reused in a subsequent reaction. Nearly quantitative recovery of catalyst (up to 98%) could be obtained from each run. As seen

in Fig. 8, the recycled catalyst could be reused six times without any additional treatment or appreciable reduction in catalytic activity. The recovered catalyst after six runs had no obvious change in structure, as shown by comparison of the FT-IR spectra to that of fresh catalyst (Fig. 9). The consistent

structure and activity of recovered and reused MNPs-PhSO₃H catalyst indicates that the reused MNPs-PhSO₃H also shows excellent performance for the synthesis of 1-amidoalkyl-1-naphthols.

Table 3. Comparison of MNPs-PhSO₃H with other catalysts reported in the literature for the synthesis of *N*-[phenyl-(2-hydroxynaphthalen-1-yl)-methyl] acetamide.^a

Entry	Catalyst (amount)	Condition	Time	Yield (%) ^b	Ref.
1	pTSA (10 mol%)	ClCH ₂ CH ₂ Cl (r.t.)	15 h	89	16
2	Montmorillonite K-10 (0.1 g)	Solvent-free (125 °C)	1.5 h	89	17
3	H ₄ SiW ₁₂ O ₄₀ (5 mol%)	Solvent-free (110 °C)	20 min	92	22
4	[TEBSA][HSO ₄] (5 mol%)	Solvent-free (120 °C)	10 min	87	33
5	Thiamin HCl (10 mol%)	EtOH (80 °C)	4 h	88	28
6	Sulfamic acid (50 mol%)	Solvent-free (30 °C)	15	88	57
7	Silica sulfuric acid (0.02g)	Solvent-free (r.t.)	2 h	85	58
8	Fe(HSO ₄) ₃ (5 mol%)	Solvent-free (85 °C)	65 min	83	19
9	I ₂ (5 mol%)	Solvent-free (125 °C)	4.5 h	87	18
10	Molybdophosphoric Acid (0.12 g)	Ethylacetate (65 °C)	3.5	94	59
11	K ₅ CoW ₁₂ O ₄₀ ·3H ₂ O (1 mol%)	Solvent-free (125 °C)	2 h	90	60
12	DPA (10 mol%)	Solvent-free (90 °C)	20 min	88	23
13	MNPs-PhSO ₃ H (0.02 g)	Solvent-free (120 °C)	40	94	This work

^a Reaction conditions: β -naphthol (1 mmol), benzaldehyde (1 mmol), and acetamide (1.2 mmol).

^b Isolated yields.

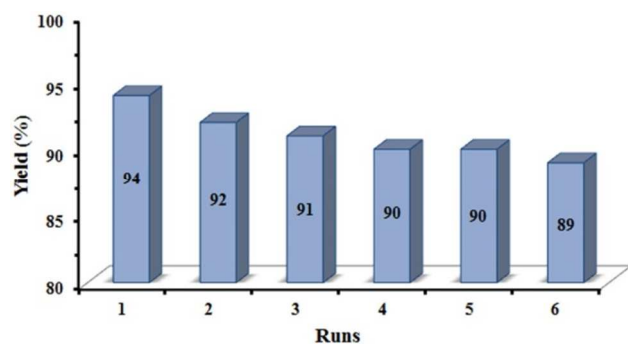


Fig. 8 Recyclability of MNPs-PhSO₃H in the reaction of 3-nitrobenzaldehyde (1 mmol), 2-naphthol (1 mmol), *N*-methylurea (1.2 mmol) and catalyst (0.02 g) under solvent-free conditions.

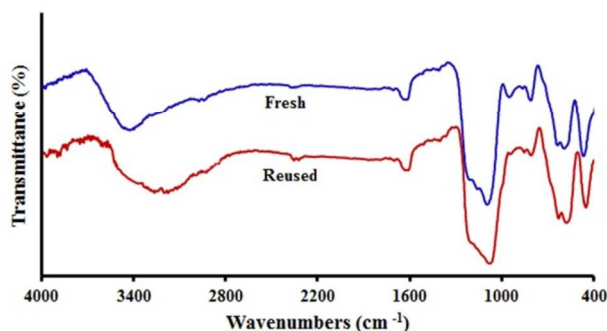


Fig. 9 FT-IR spectra of the fresh catalyst and the six-times reused catalyst.

3. Experimental

All chemicals were purchased from Merck or Fluka chemical companies and used without further purification. Melting points were measured by using capillary tubes on an electro thermal digital apparatus and are uncorrected. Known products were identified by comparison of their melting points and spectral data with those reported in the literature. Thin layer chromatography (TLC) was performed on UV active aluminum-backed plates of silica gel (TLC Silica gel 60 F₂₅₄). FTIR spectra were recorded on a Unicam Galaxy Series FT-IR 5000 spectrophotometer in the region 4000-400 cm⁻¹ using pressed KBr discs. The ¹H and ¹³C NMR spectra were recorded on a Bruker Avance spectrometer operating at 300 and 75 MHz for ¹H and ¹³C NMR, respectively in DMSO-d₆ with TMS as an internal standard. X-ray diffraction (XRD) was performed on Philips X-Pert (Cu-K α radiation, $\lambda = 0.15405$ nm) over the range 2 $\theta = 20^\circ$ -80 $^\circ$ using 0.04 $^\circ$ as the step length. Thermal gravimetric analysis (TGA) and differential thermal gravimetric (DTG) data for MNPs-PhSO₃H were recorded on a Mettler TA4000 System under an N₂ atmosphere at a heating rate of 10 °C min⁻¹. The magnetization and hysteresis loop were measured at room temperature using a Vibrating Sample Magnetometer (Model 7300 VSM system, Lake Shore Cryotronic, Inc., Westerville, OH, USA). The scanning electron microscope measurement was carried out on a Hitachi S-4700 field emission-scanning electron microscope (FE-SEM). Transmission electron microscopy (TEM) measurements were carried out on a Philips CM10 analyzer operating at 150 kV.

3.1. Preparation of the magnetic Fe₃O₄ nanoparticles (MNPs)

Fe₃O₄-MNPs were prepared using simple chemical co-precipitation described in the literature.⁶¹ Briefly, FeCl₂·4H₂O (0.9941 g, 5 mmol) and FeCl₃·6H₂O (2.7029 g, 10 mmol) were dissolved in 100 mL of deionized water in a three-necked round bottomed flask (250 mL). The mixture was heated under N₂ at 80 °C for 1h, and then 10 mL of concentrated ammonia (25%) were added quickly. The solution was stirred under N₂ for another 1 h and then cooled to room temperature. The black precipitate formed was isolated by magnetic decantation, exhaustively washed with double-distilled water until

neutrality, and further washed twice with ethanol and dried at 60 °C under vacuum.

3.2. Synthesis of Silica-Coated MNPs ($\text{Fe}_3\text{O}_4@\text{SiO}_2$ MNPs)

The $\text{Fe}_3\text{O}_4@\text{SiO}_2$ core-shell nanoparticles were prepared according to the Stöber method.⁴⁶ The details are as follows: Magnetic nanoparticles MNPs (1.0 g) were homogeneously dispersed by ultrasonic vibration in a mixture of 40 mL of ethanol, 6 mL of deionised water, and 1.5 mL of 25 wt% concentrated aqueous ammonia solution, followed by the addition of 1.4 mL of tetraethylorthosilicate (TEOS). After stirring for 12 h at room temperature under an N_2 atmosphere, the black precipitate ($\text{Fe}_3\text{O}_4@\text{SiO}_2$) was collected from the solution using a magnet, and then washed several times with water and ethanol and dried at 25 °C under vacuum.

3.3. Synthesis of 3-chloropropyl-functionalized magnetic silica nanoparticles ($\text{Fe}_3\text{O}_4@\text{SiO}_2\text{-Cl}$ MNPs)

Chloropropyl-modified silica-coated magnetic nanoparticles were prepared according to the reported procedure.⁶² In a typical procedure, 1.0 g of $\text{Fe}_3\text{O}_4@\text{SiO}_2$ MNPs were dispersed in 50 mL of dry toluene using an ultrasonic bath to produce a uniform suspension, to which 2.0 g of 3-chloropropyl-trimethoxysilane (CPTS) was added using a syringe. The resulting mixture was stirred for 48 h at 60 °C under an N_2 atmosphere. Finally, the chloropropyl-functionalized solid $\text{Fe}_3\text{O}_4@\text{SiO}_2\text{-Cl}$ MNPs were washed with toluene, separated using a magnet, and dried under vacuum.

3.4. Sulfanilic acid-functionalized silica-coated magnetic nanoparticles (MNPs- PhSO_3H)

The MNPs- PhSO_3H magnetic nanoparticles were prepared according to the method of Adama et al.⁶³ 1g of $\text{Fe}_3\text{O}_4@\text{SiO}_2\text{-Cl}$ nanoparticles were dispersed in 50 mL dry toluene by sonication over 1 h. To this suspension, 2 g (11.5 mmol) of sulfanilic acid was added, followed by 1.6 mL (11.5 mmol) of triethylamine acting as a proton scavenger. Then, the reaction mixture was refluxed for 2 days under nitrogen. The solid material was obtained by magnetic separation and washed with toluene, dichloromethane and finally with acidified ethanol followed by drying at 80 °C for 6 h under vacuum.

3.5. Acidity of MNPs- PhSO_3H

The concentration of sulfonic acid groups was quantitatively estimated by back titration using HCl (0.01 N). 2 mL of KOH (0.01 N) was added to 0.02 g of the magnetic nanoparticles and the mixture was stirred for 30 min. The catalysts were magnetically separated and washed with deionized water. The excess amount of KOH was titrated with HCl (0.01 N) in the presence of phenolphthalein as indicator. Averages of 3 separate titrations were performed to obtain an average value for the acid amount of MNPs- PhSO_3H . The results revealed that the samples of MNPs- PhSO_3H possessed 0.65 mmol g^{-1} acid amount.

3.6. General Procedure for the Synthesis of 1-Amido or aminoalkyl-2-naphthols

MNPs- PhSO_3H (0.02 g) were added as a catalyst to a mixture of β -naphthol (1 mmol), an aldehyde (1 mmol), and an amide or an amine (1.2 mmol). The mixture was magnetically stirred under thermal solvent-free condition on a preheated oil bath at 120 °C for the appropriate time. After completion of the reaction, as indicated by TLC, the resulting solidified mixture was diluted with hot THF (10

mL) and the catalyst easily separated by an external magnet. The solvent was then evaporated; the remaining solid product was recrystallized from aqueous ethanol.

3.7. Characterization data for new compounds

3.7.1. 1-(phenyl(pyridin-2-ylamino)methyl)naphthalen-2-ol (6r):

IR (KBr): ν_{max} = 3370, 3061, 1607, 1570, 1512, 1449, 1331, 1275, 1235, 1163, 1063, 999, 812, 747, 696, 637 cm^{-1} ; ^1H NMR (300 MHz, DMSO-d_6): δ = 10.00 (s, 1H), 8.45 (d, J = 8.4, 1H), 7.82-7.75 (m, 3H), 7.36 (t, J = 7.4, 1H), 7.28-7.21 (m, 6H), 7.17-7.13 (m, 6H); ^{13}C NMR (75 MHz, DMSO-d_6): δ = 169.2, 153.1, 153.9, 142.6, 132.3, 129.2, 128.5, 128.4, 127.9, 126.3, 126.0, 125.9, 123.3, 123.2, 122.3, 118.8, 118.7, 118.4, 118.3, 47.7; Anal Calcd for $\text{C}_{22}\text{H}_{18}\text{N}_2\text{O}$: C, 80.96; H, 5.56; N, 8.58. Found: C, 80.89; H, 5.61; N, 8.51.

3.7.2. 1-((4-chlorophenyl)(pyridin-2-ylamino)methyl)naphthalen-2-ol (6s):

IR (KBr): ν_{max} = 3410, 3063, 1615, 1568, 1516, 1437, 1329, 1273, 1155, 1089, 1013, 955, 885, 820, 768 cm^{-1} ; ^1H NMR (300 MHz, DMSO-d_6): δ = 10.23 (s, 1H), 7.97-7.93 (m, 2H), 7.81-7.76 (m, 2H), 7.41-7.36 (m, 2H), 7.30-7.21 (m, 8H), 6.82 (d, J = 8.4 Hz, 1H), 6.52 (t, J = 6.1 Hz, 1H); ^{13}C NMR (75 MHz, DMSO-d_6): δ = 158.3, 153.0, 147.2, 143.0, 136.8, 132.2, 130.2, 129.2, 128.5, 128.0, 127.7, 126.3, 123.6, 122.4, 119.7, 118.6, 118.4, 112.3, 109, 49.1; Anal Calcd for $\text{C}_{22}\text{H}_{17}\text{ClN}_2\text{O}$: C, 73.23; H, 4.75; N, 7.76. Found: C, 73.26; H, 4.81; N, 7.73.

3.7.3. 1-(((4-chloro-6-methylpyrimidin-2-yl)amino)(phenyl)methyl)naphthalen-2-ol (6t):

IR (KBr): ν_{max} = 3381, 3063, 2998, 1628, 1572, 1514, 1437, 1360, 1290, 1211, 1132, 895, 814, 742, 698 cm^{-1} ; ^1H NMR (300 MHz, DMSO-d_6): δ = 10.26 (s, 1H), 8.09 (d, J = 7.8, 1H), 7.83-7.76 (m, 3H), 7.45-7.18 (m, 9H), 6.65 (s, 1H), 2.25 (s, 3H); ^{13}C NMR (75 MHz, DMSO-d_6): δ = 170.5, 162.1, 160.6, 153.6, 142.9, 132.7, 129.8, 129.1, 128.8, 128.6, 128.5, 127.2, 126.8, 126.5, 123.1, 119.5, 119.1, 109.5, 50.8, 24.1; Anal Calcd for $\text{C}_{22}\text{H}_{18}\text{ClN}_3\text{O}$: C, 70.30; H, 4.83; N, 11.18. Found: C, 70.37; H, 4.93; N, 11.14.

3.7.4. 1-(((4-chloro-6-methylpyrimidin-2-yl)amino)(4-chlorophenyl)methyl)naphthalen-2-ol (6u):

IR (KBr): ν_{max} = 3379, 3059, 2992, 1628, 1572, 1516, 1437, 1358, 1289, 1269, 1211, 1092, 1014, 899, 814, 742 cm^{-1} ; ^1H NMR (300 MHz, DMSO-d_6): δ = 10.28 (s, 1H), 8.05 (d, J = 7.4, 1H), 7.82-7.75 (m, 3H), 7.46-7.27 (m, 8H), 6.66 (s, 1H), 2.25 (s, 3H); ^{13}C NMR (75 MHz, DMSO-d_6): δ = 171.0, 161.9, 157.5, 154.5, 153.9, 141.9, 140.2, 132.5, 131.9, 130.8, 130.0, 129.3, 128.6, 128.4, 128.1, 123.3, 118.4, 116.9, 99.4, 50.4, 18.8; Anal Calcd for $\text{C}_{22}\text{H}_{17}\text{Cl}_2\text{N}_3\text{O}$: C, 64.40; H, 4.18; N, 10.24. Found: C, 64.44; H, 4.23; N, 10.28.

3.7.5. 1-((2-chloro-6-fluorophenyl)((4-chloro-6-methylpyrimidin-2-yl)amino)methyl)naphthalen-2-ol (6v):

IR (KBr): ν_{max} = 3420, 3065, 2996, 1630, 1572, 1518, 1437, 1373, 1290, 1269, 1238, 1175, 1101, 1057, 950, 897, 808, 775, 741 cm^{-1} ; ^1H NMR (300 MHz, DMSO-d_6): δ = 9.91 (s, 1H), 8.10 (d, J = 7.5, 1H), 7.81-7.77 (m, 3H), 7.44-7.08 (m, 7H), 6.63 (s, 1H), 2.23 (s, 3H); ^{13}C NMR (75 MHz, DMSO-d_6): δ = 171.5, 157.7, 154.7, 154.2, 133.6, 132.5, 131.0, 129.8, 129.3, 128.4, 127.4, 126.3, 126.2, 123.0, 122.8, 122.4, 119.0, 115.9, 115.3, 98.7, 48.4, 18.8; Anal Calcd for $\text{C}_{22}\text{H}_{16}\text{Cl}_2\text{FN}_3\text{O}$: C, 61.70; H, 3.77; N, 9.81. Found: C, 61.66; H, 3.84; N, 9.83.

3.7.6. 1-(((4-chloro-6-methylpyrimidin-2-yl)amino)(2-chlorophenyl)methyl)naphthalen-2-ol (6w):

IR (KBr): ν_{\max} = 3421, 3057, 2990, 1630, 1572, 1528, 1440, 1359, 1288, 1271, 1211, 1122, 1067, 897, 816, 775, 742 cm^{-1} ; ^1H NMR (300 MHz, DMSO- d_6): δ = 10.04 (s, 1H), 8.12 (s, 1H), 8.01 (d, J = 7.1, 1H), 7.76 (t, J = 7.5, 2H), 7.53 (s, 1H), 7.42-7.15 (m, 8H), 6.61 (s, 1H), 2.22 (s, 3H); ^{13}C NMR (75 MHz, DMSO- d_6): δ = 171.4, 157.6, 154.3, 138.1, 137.0, 132.5, 130.8, 130.1, 129.9, 129.5, 129.2, 128.5, 127.2, 123.2, 122.6, 122.1, 118.9, 115.7, 114.8, 98.8, 49.9, 18.9; Anal Calcd for $\text{C}_{27}\text{H}_{17}\text{Cl}_3\text{N}_3\text{O}$: C, 64.4; H, 4.18; N, 10.24. Found: C, 64.33; H, 4.24; N, 10.16.

4. Conclusions

In conclusion, a new magnetic organic-inorganic nanocomposite (MNPs- PhSO_3H) was prepared by a very simple and inexpensive method, and was characterized by FT-IR, XRD, TG-DTG, FE-ESM, EDS, TEM, VSM and acid-base titration. This catalyst has been successfully applied in a one-pot three-component condensation of amide/amine/urea with aldehyde and 2-naphthol under solvent-free conditions to prepare 1-amido or 1-aminoalky-2-naphthols in high yields (up to 96%). High catalytic activity, generality, high yields, short reaction times and the simple experimental procedure combined with the ease of work-up of the product make this method convenient and environmentally benign for synthesis of 1-amido- or 1-aminoalky-2-naphthols. The present method is applicable to a wide variety of aldehydes, and amides or urea or amines for the synthesis of corresponding 1-amido or 1-aminoalky-2-naphthols. Moreover, the catalyst is stable under the reaction conditions and can be readily separated by use of a magnet and reused without any significant loss of catalytic activity after six runs.

Acknowledgement

We gratefully acknowledge financial support from the Research Council of Arak University.

References

- ^a Department of Chemistry, Dezful Branch, Islamic Azad University, Dezful, Iran
- ^b Department of Chemistry, Faculty of Science, Arak University, Arak 38156-8-8349, Iran
- ^c School of Applied Sciences, Auckland University of Technology, Private Bag 92006, Auckland 1142, New Zealand
1. A. Strecker, *Leibigs Ann. Chem.*, 1850, **75**, 27-45.
2. N. K. Terret, M. Gardener, D. W. Gordon, R. J. Kobylecki and J. Steele, *Tetrahedron*, 1995, **51**, 8135-8173.
3. L. A. Thomson and J. A. Ellman, *Chem. Rev.*, 1996, **96**, 555-600.
4. A. Domling and I. Ugi, *Angew. Chem. Int. Ed.*, 2000, **39**, 3168-3210.
5. N. Ahmed and J. E. van Lie, *Tetrahedron Lett.*, 2007, **48**, 5407-5409.
6. A. Domling, *Chem. Rev.*, 2006, **106**, 17-89.
7. M. Kidwai and R. Chauhan, *J. Mol. Catal. A: Chem.*, 2013, **377**, 1-6.
8. A. Hasaninejad, S. Firoozi and F. Mandegani, *Tetrahedron Lett.*, 2013, **54**, 2791-2794.
9. S. Knapp, *Chem. Rev.*, 1995, **95**, 1859-1876.
10. D. Seebach and J. L. Matthews, *Chem. Commun.*, 1997, 2015-2022.
11. E. Juaristi, *In Enantioselective Synthesis of β -Aminoacids*, John Wiley & Sons, New York, 1997.
12. A. Y. Shen, C. T. Tsai and C. L. Chen, *Eur. J. Med. Chem.*, 1999, **34**, 877-882.

13. T. Dingermann, D. Steinhilber and G. Folkes, *Molecular Biology in Medicinal Chemistry*, Wiley-VCH, 2004.
14. R. Hulst, H. Heves, N. C. M. W. Peper and R. M. Kellogg, *Tetrahedron: Asymmetry* 1996, **7**, 1373-1384.
15. X. Li, C.-H. Yeung, A. S. C. Chan and T.-K. Yang, *Tetrahedron: Asymmetry*, 1999, **10**, 759-763.
16. M. M. Khodaei, A. R. Khosropour and H. Moghanian, *Synlett*, 2006, 916-920.
17. S. Kantavari, S. V. N. Vuppalapati and L. Nagarapu, *Catal. Commun.*, 2007, **8**, 1857-1862.
18. B. Das, K. Laxminarayana, B. Ravikanth and B. R. Rao, *J. Mol. Catal. A: Chem.*, 2007, **261**, 180-183.
19. H. R. Shaterian, H. Yarahmadi and M. Ghashang, *Bioorg. Med. Chem. Lett.*, 2008, **18**, 788-792.
20. R. Ghorbani-Vaghei and S. M. Malaekhepour, *Cent. Eur. J. Chem.*, 2010, **8**, 1086-1089.
21. M. Wang, Y. Liang, T. T. Zhang and J. J. Gao, *Chem. Nat. Compd.*, 2012, **48**, 185-188.
22. A. R. Supale and G. S. Gokavi, *J. Chem. Sci.*, 2010, **122**, 189-192.
23. M. Zandi and A. R. Sardarian, *C.R. Chimie*, 2012, **15**, 365-369.
24. G. H. Mahdavinia and M. A. Bigdeli, *Chin. Chem. Lett.*, 2009, **20**, 383-386.
25. M. Wang, Y. Liang, T. T. Zhang and J. J. Gao, *Chin. Chem. Lett.*, 2012, **23**, 65-68.
26. H. Hashemi and A. R. Sardarian, *J. Iran. Chem. Soc.*, 2013, **10**, 745-750.
27. G. C. Nandi, S. Samai, R. Kumar and M. S. Singh, *Tetrahedron Lett.*, 2009, **50**, 7220-7222.
28. M. Lei, L. Ma and L. Hu, *Tetrahedron Lett.*, 2009, **50**, 6393-6397.
29. H. R. Shaterian, H. Yarahmadi and M. Ghashang, *Tetrahedron*, 2008, **64**, 1263-1269.
30. S. B. Patil, P. R. Singh, M. P. Surpur and S. D. Samant, *Synth. Commun.*, 2007, **37**, 1659-1664.
31. G. Srihari, M. Nagaraju and M. M. Murthy, *Helv. Chim. Acta.*, 2007, **90**, 1497-1504.
32. D. Kundu, A. Majee and A. Hajra, *Catal. Commun.*, 2010, **11**, 1157-1159.
33. A. R. Hajipour, Y. Ghayeb, N. Sheikhan and A. E. Ruoho, *Tetrahedron Lett.*, 2009, **50**, 5649-5651.
34. L. Han, H. Ji Choi, S. Jin Choi, B. Liub and D. Won Park, *Green Chem.*, 2011, **13**, 1023-1028.
35. L. Han, S. W. Park and D. W. Park, *Energy Environ. Sci.*, 2009, **2**, 1286-1292.
36. S. R. Jagtap, V. P. Raje, S. D. Samant and B. M. Bhanage, *J. Mol. Catal. A: Chem.*, 2007, **266**, 69-72.
37. J. Sun, S. Fujita, F. Zhao and M. Araj, *Green Chem.*, 2004, **6**, 613-616.
38. B. Rac, A. Molnar, P. Forgo, M. Mohai and I. Bertoti, *J. Mol. Catal. A Chem.*, 2006, **244**, 46-57.
39. M. A. Nasserri and M. Sadeghzadeh, *J. Chem. Sci.*, 2013, **125**, 537-544.
40. S. Safaei, I. Mohammadpoor-Baltork, A. R. Khosropour, M. Moghadam, S. Tangestaninejad and V. Mirkhani, *Catal. Sci. Technol.*, 2013, **3**, 2717-2722.
41. V. Polshettiwar, R. Luque, A. Fihri, H. Zhu, M. Bouhrara and J. M. Basset, *Chem. Rev.*, 2011, **111**, 3036-3075.

42. S. Shylesh, V. Schunemann and W. R. Thiel, *Angew. Chem., Int. Ed.*, 2010, **49**, 3428-3459.
43. D. K. Yi, S. S. Lee and J. Y. Ying, *Chem. Mater.*, 2006, **18**, 2459-2461.
44. Y. H. Leng, K. Sato, Y. G. Shi, J. G. Li, T. Ishigaki, T. Yoshida and H. Kamiya, *J. Phys. Chem. C*, 2009, **113**, 16681-16685.
45. A. L. Morel, S. I. Nikitenko, K. Gionnet, A. Wattiaux, J. Lai-Kee-Him, C. Labrugere, B. Chevalier, G. Deleris, C. Petibois, A. Brisson and M. Simonoff, *ACS Nano*, 2008, **2**, 847-856.
46. W. Stöber, A. Fink and E. J. Bohn, *J. Colloid Interface Sci.*, 1968, **26**, 62-69.
47. G. Feng, D. Hu, L. Yang, Y. Cui, X. Cui and H. Li, *Sep. Purif. Technol.*, 2010, **74**, 253-260.
48. J. Giri, S. G. Thakurta, J. Bellare, A. K. Nigam and D. Bahadur, *J. Magn. Magn. Mater.*, 2005, **293**, 62-68.
49. K. Petcharoena and A. Sirivat, *Mater. Sci. Eng. B*, 2012, **177**, 421-424.
50. D. A. Kotadia and S. S. Soni, *J. Mol. Catal. A: Chem.*, 2012, **354**, 44-49.
51. J. Safari and Z. Zarnegar, *J. Mol. Catal. A: Chem.*, 2013, **379**, 269-276.
52. M. A. Zolfigol, A. Khazaei, A. R. Moosavi-Zare, A. Zare and V. Khakyzadeh, *Appl. Catal. A: Gen.*, 2011, **400**, 70-81.
53. A. Shahrissa, S. Esmati and M. Gholamhosseini Nazari, *J. Chem. Sci.*, 2012, **124**, 927-931.
54. H. Alinezhad, M. Tajbakhsh, M. Norouzi, S. Bagheri and M. Akbari, *C. R. Chimie*, 2014, **17**, 7-11.
55. H. Jafari and H. Moghanian, *Lett. Org. Chem.*, 2012, **9**, 273-275.
56. S. B. Patil, P. R. Singh, M. P. Surpur and S. D. Samant, *Ultrasonics Sonochemistry*, 2007, **14**, 515-518.
57. R. R. Nagawade and D. B. Shinde, *Chin. J. Chem.*, 2007, **25**, 1710-1714.
58. M. Z. Kassaei, H. Masrouri and F. Movahedi, *Appl. Catal. A: Gen.*, 2011, **395**, 28-33.
59. W.-Q. Jiang, L.-T. An and J.-P. Zou, *Chin. J. Chem.*, 2008, **26**, 1697-1701.
60. L. Nagarapu, M. Baseeruddin, S. Apuri and S. Kantevari, *Catal. Commun.*, 2007, **8**, 1729-1734.
61. K. Can, M. Ozmen and M. Ersoz, *Colloids Surf. B* 2009, **71**, 154-159.
62. T. Zeng, L. Yang, R. Hudson, G. Song, A.-R. Moores and C.-J. Li, *Org. Lett.*, 2011, **13**, 442-445.
63. F. Adama, K. Mohammed Hello and T. Hussein Ali, *Appl. Catal. A: Gen.*, 2011, **399**, 42-49.

Graphical Abstract:

Sulfanilic acid-functionalized silica-coated magnetite nanoparticles as an efficient, reusable and magnetically separable catalyst for the solvent-free synthesis of 1-amido- and 1-aminoalkyl-2-naphthols

Hassan Moghanian,^{*} Akbar Mobinikhaledi, Allan G. Blackman, Elaheh Sarough-Farahani

